Reaction-Induced Microphase Separation in Epoxy Thermosets Containing Poly(ϵ-caprolactone)-*block*-poly(*n*-butyl acrylate) Diblock Copolymer

Zhiguang Xu and Sixun Zheng*

Department of Polymer Science and Engineering, Shanghai Jiao Tong University, Shanghai 200240, P. R. China

Received October 27, 2006; Revised Manuscript Received January 29, 2007

ABSTRACT: Reaction-induced microphase separation in epoxy thermosets containing an amphiphilic diblock copolymer was investigated in this work. To this end, the diblock copolymer poly(ϵ-caprolactone)-*block*-poly(*n*-butyl acrylate) (PCL-*b*-PBA) was synthesized via the combination of ring-opening polymerization (ROP) and atom transfer radical polymerization (ATRP). The block copolymer was incorporated into epoxy thermosets. Before the curing reaction all the subchains of the diblock copolymer were miscible with the precursors of epoxy resin. After curing, only the PBA blocks were separated out whereas the PCL blocks remained miscible with epoxy resin. Such a reaction-induced microphase separation results in the formation of ordered nanostructures in the thermosets. The nanostructures in the thermosets were investigated by means of field emission scanning electron microscopy (FESEM), atomic force microscopy (AFM), small-angle X-ray scattering (SAXS), and dynamic mechanical analysis (DMA). It is found that, depending on the concentration of the diblock copolymer, the thermosets can displayed spherical particles or lamellar nanostructures. The SAXS curves with the multiple scattering maxima suggests that the thermosets possess long-range ordered nanostructures.

Introduction

Reaction-induced phase separation (RIPS) in thermosets has been extensively investigated during the past decades.[1] The goal of the studies is to improve the mechanical properties of thermosets by controlling the morphology of thermosetting polymer blends. Generally, the thermosetting polymer blends are prepared starting from a homogeneous solution of modifier (e.g., thermoplastics or elastomers) with precursors of thermosets, and phase separation would occur with polymerization proceeding. The driving force for RIPS is ascribed to the unfavorable entropic contribution to the mixing free energy due to the molecular weight of infinity for cross-linked components. Nonetheless, the miscible thermosetting blends will be obtained if the favorable intermolecular specific interactions (e.g., hydrogen bonding) are present between these linear polymers and thermosets.[1b,2] For instance, poly(ethylene oxide) (PEO) and poly(ϵ-caprolactone) (PCL) have been reported to be miscible with epoxy thermosets cured with aromatic amine due to the formation of the intermolecular hydrogen bonding interactions.[2]

Generally, reaction-induced phase separation occurs on the macroscopic scale while modifiers are some linear homopolymers or random copolymers. It is of great interest to investigate the phase behavior to thermosetting polymer blends with an amphiphilic diblock copolymer. If one block of the amphiphilic diblock copolymer is miscible, another one became immiscible with the thermosets; i.e., reaction-induced microphase separation (RIMPS) occurs. Nonetheless, RIMPS is quite different from the reaction-induced phase separation in the blends of thermosets with linear homopolymers or random copolymers. Because of the presence of the miscible blocks, RIMPS occurs on the nanometer scale and the thermosets could display nanostructured morphology.[3]

* To whom correspondence should be addressed: e-mail szheng@sjtu.edu.cn; Tel 86-21-54743278; Fax 86-21-54741297.

It should be pointed out that Bates et al.[4] have precedently proposed the strategy of self-assembly to access the nanostructures of thermosets; i.e., the precursors of thermosets act as the selective solvents of block copolymers, and some self-assembly nanostructures such as lamellar, bicontinuous, cylindrical, and spherical structures are formed in the mixtures depending on the blend composition before curing reaction. These preformed nanostructures are fixed through the subsequent curing reaction although there are some small changes in the nanostructures after and before curing reaction.[4] Mechanistically, there is a significant difference between self-assembly and RIMPS approaches. In the self-assembly approach, the formation of micelle structures of block copolymer in selective solvents is governed by the equilibrium thermodynamics of the multicomponent system. Nonetheless, the formation of nanostructures via RIMPS could be greatly influenced by the competitive kinetics between polymerization and phase separation.[1] With the reaction proceeding, a series of structural changes involving chain extension, branching, and cross-linking occurred in succession; i.e., the system undergoes the sol−gel transition within a short time. It is of importance to investigate the formation of nanostructures in thermosets via the RIMPS approach for the morphological control of thermosets on the nanometer scale. However, the studies remain largely unexplored vis-à-vis the self-assembly approach.[4,5]

The purpose of this work is to show that ordered nanostructures could be accessed via the RIMPS approach. To the best of our knowledge, lamellar nanostructures have not obtained via the RIMPS approach. To this end, a new amphiphilic diblock copolymer, poly(ϵ-caprolactone)-*block*-poly(*n*-butyl acrylate) (PCL-*b*-PBA), was synthesized by knowing that PCL is miscible with epoxy thermosets[10] whereas PBA will undergo reaction-induced phase separation in epoxy thermosets. It is expected that the nanostructured epoxy thermosets can be prepared via the so-called reaction-induced microphase separation in this system. In this work, field emission scanning electron micros-

10.1021/ma062486v CCC: $37.00
Published on Web 03/01/2007

copy (FESEM), atomic force microscopy (AFM), and small-angle X-ray scattering (SAXS) are used to examine the ordered nanostructures formed via the reaction-induced microphase separation. Differential scanning calorimetry (DSC) and dynamic mechanical analysis (DMA) were used to investigate the glass transition behavior of the nanostructures.

Experimental Section

Materials. Diglycidyl ether of bisphenol A (DGEBA) with epoxide equivalent weight of 185−210 was purchased from Shanghai Resin Co., China. 4,4′-Methylenebis(2-chloroaniline) (MOCA), benzyl alcohol, *n*-butyl acrylate (BA), and copper(I) bromide were of analytically pure grade, obtained from Shanghai Reagent Co., China. ϵ-Caprolactone (CL) (99%) was purchased from Fluka Co., Germany, and it was dried over calcium hydride (CaH_2) and distilled under decreased pressure. Stannous octanoate [$Sn(Oct)_2$] was purchased from Aldrich Co. Prior to use, *n*-butyl acrylate (BA) was washed with 5% aqueous NaOH and deionized water for three times and then was distilled over CaH_2 under reduced pressure. *N*,*N*,*N*′,*N*″,*N*‴-Pentamethyldiethylenetriamine (PMDETA) (Aldrich, 99%), 2-bromoisobutyl bromide (Aldrich, 97%), and methyl 2-bromopropionate (Aldrich, >99%) were used as received. Copper(I) bromide was purified according to the literature procedure.[6] Before use, xylene and tetrahydrofuran (THF) were dried by reflux over sodium and then distilled.

Synthesis of Monohydroxyl-Terminated Poly(ϵ-caprolactone) (PCL-OH). Monohydroxyl-terminated poly(ϵ-caprolactone) (PCL-OH) was synthesized via the ring-opening polymerization (ROP) of ϵ-CL with benzyl alcohol as the initiator and $Sn(Oct)_2$ was used as the catalyst. Typically, benzyl alcohol (0.3643 g, 3.37 mmol) and ϵ-CL (20.0000 g, 175.4 mmol) were charged to a 100 mL round-bottom flask equipped with a dry magnetic stirring bar and $Sn(Oct)_2$ (1/1000 wt with respect to ϵ-CL) was added using a syringe. The flask was connected to a standard Schlenk line, and the reactive mixture was degassed via three pump−freeze−thaw cycles and then immersed in a thermostated oil bath at 120 °C for 24 h. The crude product was dissolved in tetrahydrofuran, and the solution was dropped into an excessive amount of petroleum ether to afford the procipitates; this procedure was repeated three times to obtain white solids. The product was dried in a vacuum oven until a constant weight was obtained with a yield of 96%. The molecular weight of PCL-OH was determined by means of ^{1}H NMR spectroscopy. The molecular weight of the PCL-OH was calculated according to the ratio of integration intensity of aliphatic methylene protons to aromatic protons to be $M_n = 5700$.

Preparation of PCL-*b*-PBA. In order to synthesize PCL-*b*-PBA diblock copolymer by means of atom transfer radical polymerization (ATRP), poly(ϵ-caprolactone) macroinitiator was first prepared by following the literature method.[7] The above PCL-OH was used to react with 2-bromoisobutyryl bromide in the presence of triethylamine to afford the 2-bromoisobutyryl-terminated PCL [PCL-$OOCCBr(CH_3)_2$]. The poly(ϵ-caprolactone)-*block*-poly(*n*-butyl acrylate) (PCL-*b*-PBA) diblock copolymer was synthesized by means of atom transfer radical polymerization (ATRP) with the 2-bromoisobutyryl-terminated PCL as a macroinitiator. In a typical experiment, the PCL macroinitiator (5.000 g, 0.862 mmol), Cu(I)-Br (0.1237 g, 0.862 mmol), PMDETA (180 μL, 0.862 mmol), 15 mL of anhydrous xylene, and *n*-BA (15.000 g, 117 mmol) were charged to a 100 mL round-bottom flask. The system was connected to the Schlenk line system, and three freeze−pump−thaw cycles were used to remove the trace of moisture and oxygen. The reactive system was immersed into an oil bath at 90 °C for 10 h. The crude product was dissolved in tetrahydrofuran and passed through a neutral alumina column to remove the catalyst; the polymer solution was dropped into an excessive amount of cold methanol. The PCL-*b*-PBA diblock copolymer was dried in vacuo at room temperature for 48 h. The polymer (12.562 g) was obtained with the conversion of *n*-butyl acrylate monomer being 50.4%. The molecular weight of the block copolymer was determined by means of gel permeation chromatography (GPC) to be $M_n = 17\,900$ with $M_w/M_n = 1.07$. In view of the molecular weight of block copolymer by ^{1}H NMR, the length of PBA subchain of the block copolymer is calculated to be $M_n = 9100$.

Synthesis of PBA. The PBA with the molecular weight comparable to the length of PBA in the diblock copolymer was synthesized via atom transfer radical polymerization (ATRP), and methyl 2-bromopropionate was used as an initiator. BA (17.9500 g, 140.23 mmol), Cu(I)Br (0.1824 g, 1.27 mmol), and PMDETA (265 μL, 1.27 mmol) were charged to a 50 mL flask equipped with a magnetic stirrer, and 0.2123 g (1.27 mmol) of methyl 2-bromopropionate was added with a syringe. The system was connected to the Schlenk line system, and three freeze−pump−thaw cycles were used to remove the trace of moisture and oxygen. The polymerization was carried out at 80 °C for 7 h, and the conversion of BA was controlled within 71% and the molecular weight was determined to be $M_n = 9900$.

Preparation of DGEBA/PBA Blends. The blends of DGEBA with the PBA homopolymer were prepared by solution casting from tetrahydrofuran (THF) at room temperature. The concentration was controlled within 5% (w/v). To remove the residual solvent, all the blend films were further desiccated in a vacuum at 50 °C for 48 h.

Preparation of Binary Thermosetting Blends of Epoxy and PBA (and/or PCL). A desired amount of the PBA (and/or PCL) homopolymer was dissolved in DGEBA, and then stoichiometric MOCA with respect to DGEBA was added with continuous stirring until the mixtures were homogeneous. The ternary mixture was poured into Teflon molds and cured at 150 °C for 2 h plus 180 °C for 2 h for postcuring.

Preparation of Epoxy Thermosets Containing PCL-*b*-PBA. The diblock copolymer PCL-*b*-PBA was dissolved in DGEBA with continuous stirring, and the curing agent MOCA was added to the mixtures with vigorous stirring until homogeneous solutions were obtained. The ternary mixture was poured into Teflon molds and cured at 150 °C for 2 h plus 180 °C for 2 h for postcuring.

Measurement and Characterization. Nuclear Magnetic Resonance Spectroscopy (NMR). The samples were dissolved in deuterated chloroform, and the NMR spectra were measured on a Varian Mercury Plus 400 MHz NMR spectrometer with tetramethylsilane (TMS) as the internal reference.

Gel Permeation Chromatography (GPC). The molecular weights and molecular weight distribution of polymers were determined on a Waters 717 Plus autosampler gel permeation chromatography apparatus equipped with Waters RH columns and a Dawn Eos (Wyatt Technology) multiangle laser light scattering detector, and the measurements were carried out at 25 °C with tetrahydrofuran (THF) as the eluent at the rate of 1.0 mL/min.

Phase Contrast Microscopy (PCM). A Leica DMLP polarized optical microscope equipped with a hot stage (Linkam TH960, Linkam Scientific Instruments, Ltd. UK) with a precision of ±0.1 °C was used for the determination of cloud point temperature (T_{cp}) of DGEBA/PBA mixtures. The THF solutions of the mixtures were cast onto cover glasses; the majority of solvent was removed at 50 °C, and the residual solvent was further eliminated in vacuo at 50 °C for 2 h. The films of the blends were sandwiched between two cover glasses. To measure the cloud point curve (CPC), the blend films with various compositions were observed under a polarizing microscope in which the angle between the polarizer and analyzer was 45°.[8] The samples were heated through the cloud points at the rate of 5 °C/min; temperature was increased until a homogeneous solution was obtained. The cloud point was defined as the initial temperature of turbidity disappearance. The cloud points were plotted as a function of blend composition.

Scanning Electron Microscopy (SEM). In order to observe the phase structure of epoxy blends, the thermosets were fractured under cryogenic condition using liquid nitrogen. The fractured surfaces so obtained were immersed in THF at room temperature for 30 min. The macroscopically separated phases (if any) can be preferentially etched by the solvent while epoxy matrix phase remains unaffected. The etched specimens were dried to remove the solvents. The fracture surfaces were coated with thin layers of

Scheme 1. Synthesis of PCL-*b*-PBA Diblock Copolymer

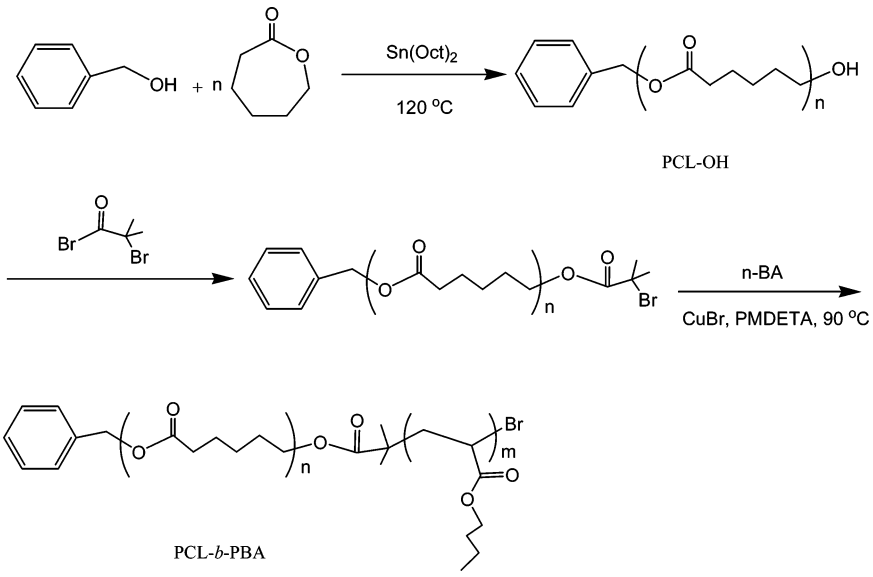

gold of about 100 Å. The thermosets containing PBA were examined with a Hitachi S210 scanning electron microscope (SEM) at an activation voltage of 15 kV while the thermosets containing PBA-*b*-PCL were observed by means of a JEOL JSM 7401F field emission scanning electron microscope (FESEM) at an activation voltage of 5 kV.

Atomic Force Microscopy (AFM). The specimens of thermosets for AFM observation were trimmed using a microtome machine, and the thickness of the specimens was about 70 nm. The morphological observation of the samples was conducted on a Nanoscope IIIa scanning probe microscope (Digital Instruments, Santa Barbara, CA) in tapping mode. A tip fabricated from silicon (125 μm in length with ca. 500 kHz resonant frequency) was used for scan, and the scan rate was 2.0 Hz.

Small-Angle X-ray Scattering (SAXS). The SAXS measurements were taken on a Bruker Nanostar system. Two-dimensional diffraction patterns were recorded using an image intensified CCD detector. The experiments were carried out at room temperature (25 °C) using Cu Kα radiation ($\lambda = 1.54$ Å, wavelength) operating at 40 kV, 35 mA. The intensity profiles were output as the plot of scattering intensity (I) vs scattering vector, $q = (4/\lambda)\sin(\theta/2)$ (θ = scattering angle).

Differential Scanning Calorimetry (DSC). The calorimetric measurements were performed on a Perkin-Elmer Pyris 1 differential scanning calorimeter in a dry nitrogen atmosphere. An indium standard was used for temperature and enthalpy calibrations. The samples (about 8.0 mg in weight) were first heated to 180 °C and held at this temperature for 3 min to remove the thermal history, followed by quenching to −70 °C. A heating rate of 20 °C/min was used at all cases. The glass transition temperature (T_g) was taken as the midpoint of the heat capacity change. The melting temperatures (T_m) were taken as the temperatures of the maximum of endothermic peak.

Dynamic Mechanical Thermal Analysis (DMTA). The dynamic mechanical tests were carried out on a TA Instruments DMA Q800 dynamic mechanical thermal analyzer (DMTA) equipped with a liquid nitrogen apparatus in a single cantilever mode. The frequency used was 1.0 Hz, and the heating rate was 3.0 °C/min. The specimen dimension was 25 × 5.0 × 2.0 mm^3. The experiments were carried out from −100 °C until the samples became too soft to be tested.

Results

Synthesis of PBA-*b*-PCL Diblock Copolymer. The synthetic route of the diblock copolymer is shown in Scheme 1. The monohydroxyl-terminated PCL block was synthesized with benzyl alcohol as the initiator via the ring-opening polymerization of ϵ-caprolactone catalyzed with Sn(Oct)$_2$. The polymerization was carried out in bulk at 120 °C for 24 h to afford the molecular weight of PCL to be $M_n = 5700$, calculated from the ratio of integration intensities of methylene (−CH$_2$−) protons of terminal benzyl group to those of PCL chain. The monohydroxyl-terminated PCL block was used to react with 2-bromoisobutyl bromide to afford the macromonomer (i.e., PCL−OOCCBr(CH$_3$)$_2$] for the atom transfer radical polymerization (ATRP) of *n*-butyl acrylate. The ATRP was performed at 90 °C for 10 h. Shown in Figure 1 is the ^{1}H NMR spectrum of the resulting polymer. The resonance at 0.93 ppm was assigned to the methyl protons of PBA whereas the peaks at 7.35 and 5.11 ppm were ascribed to the resonance of the protons of aromatic rings and methylene moiety at the PCL block ends. The GPC curves of the diblock copolymer displayed a unimodal peak, and the molecular weight was determined to be M_n = 17 900 with $M_w/M_n = 1.07$ (see Figure 2). The results of ^{1}H

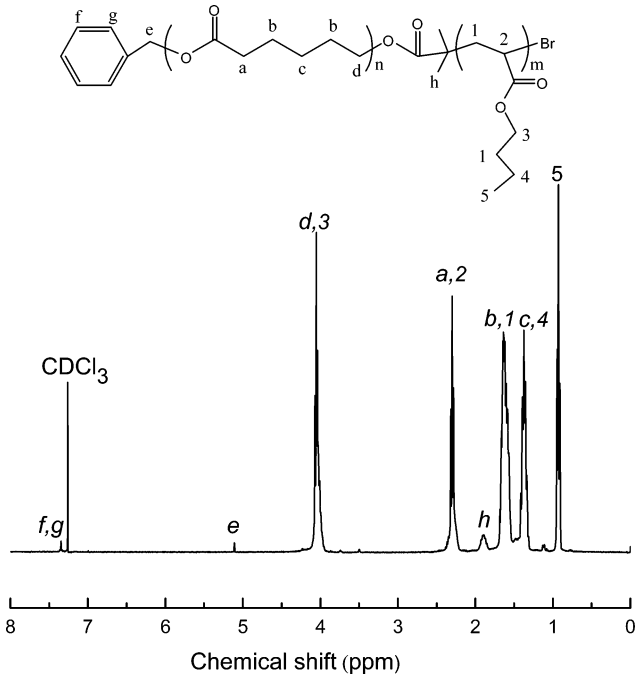

Figure 1. ^{1}H NMR spectrum of PCL-*b*-PBA diblock copolymer.

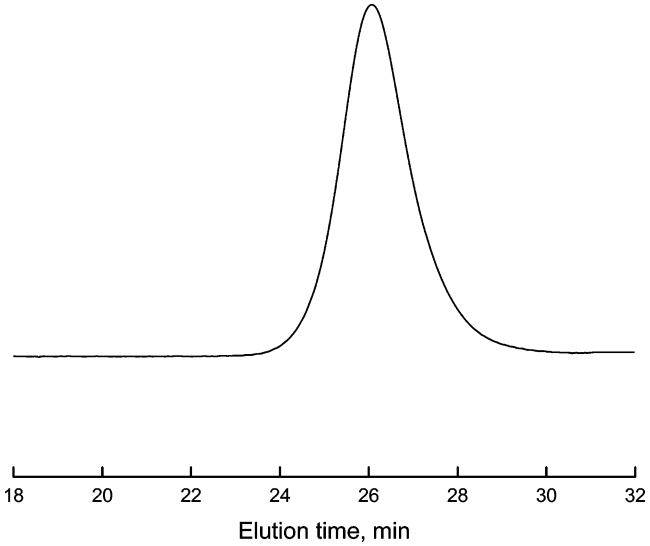

Figure 2. GPC curve of PCL-*b*-PBA.

NMR and GPC indicate that the PCL-*b*-PBA diblock copolymer was successfully obtained.

Morphology of Thermosets. The PCL-*b*-PBA diblock copolymer was used to incorporate into epoxy resin to prepare the nanostructured thermosets. Before curing, all the ternary mixtures composed of DGEBA, the curing agent (i.e., MOCA), and PCL-*b*-PBA were homogeneous and transparent, suggesting that no macroscopic phase separation occurred at the scale exceeding the wavelength of visible light at room and curing temperatures. The mixtures were cured at 150 °C for 2 h plus 180 °C for 2 h, and the epoxy thermosets were prepared with PCL-*b*-PBA diblock copolymer content up to 40 wt %. It is noted that the cured blends containing PCL-*b*-PBA less than 40 wt % are transparent whereas the thermoset containing 40 wt % of PCL-*b*-PBA became translucent after curing. The thermosets containing PBA-*b*-PCL diblock copolymer were subjected to field emission scanning electron microscopy (FESEM). Representatively shown in Figure 3 are the FESEM micrographs of the thermosets containing 10 wt % PBA-*b*-PCL, etched with THF. At the lower magnification, a featureless morphology was exhibited (Figure 3A), implying that no macroscopic phase separation occurred. Nonetheless, the nanostructured morphology was seen in the FESEM micrograph at the higher magnification (Figure 3B). It is seen that the spherical particles with the diameter of 10−20 nm were uniformly dispersed in the epoxy matrix.

In order to observe the nanostructure more clearly, the cured thermosetting blends were trimmed using an ultrathin microtome, and the sections were subjected to the morphological observations with atomic force microscopy (AFM). Shown in Figure 4 are the AFM images of the thermosets containing 10, 20, 30, and 40 wt % of the PCL-*b*-PBA diblock copolymer. The left and right images are the topography and phase contrast images, respectively. It is noted that all the thermosetting blends possess the nanostructured morphologies. In terms of the volume fraction of PBA and the difference in viscoelastic properties between epoxy and PBA phases, the light continuous regions could be ascribed to the cross-linked epoxy matrix, which was miscible with the PCL subchain of the diblock copolymer while the dark regions are assigned to PBA domains. It is seen that the PBA microphases were dispersed in the continuous epoxy matrix until the content of the diblock copolymer is 30 wt %. For the cured blend containing 10 wt % of PCL-*b*-PBA, the separate PBA particles were imbedded in the continuous epoxy matrix at the average size of ca. 10−20 nm in diameter (Figure 4a). When the content of PCL-*b*-PBA exceeds 10 wt %, the separate PBA nanophases became coagulated and some interconnected nanoobjects appeared (Figure 4b,c). With increasing the content of the diblock copolymer, lamellar nanostructures appeared besides the interconnected nanoobjects, as indicated by "A" and "B" in Figure 4d together with Figure 5A,B. The lamellar nanostructures exhibited the feature of long-range order, which was confirmed by the results of small-angle X-ray scattering (SAXS).

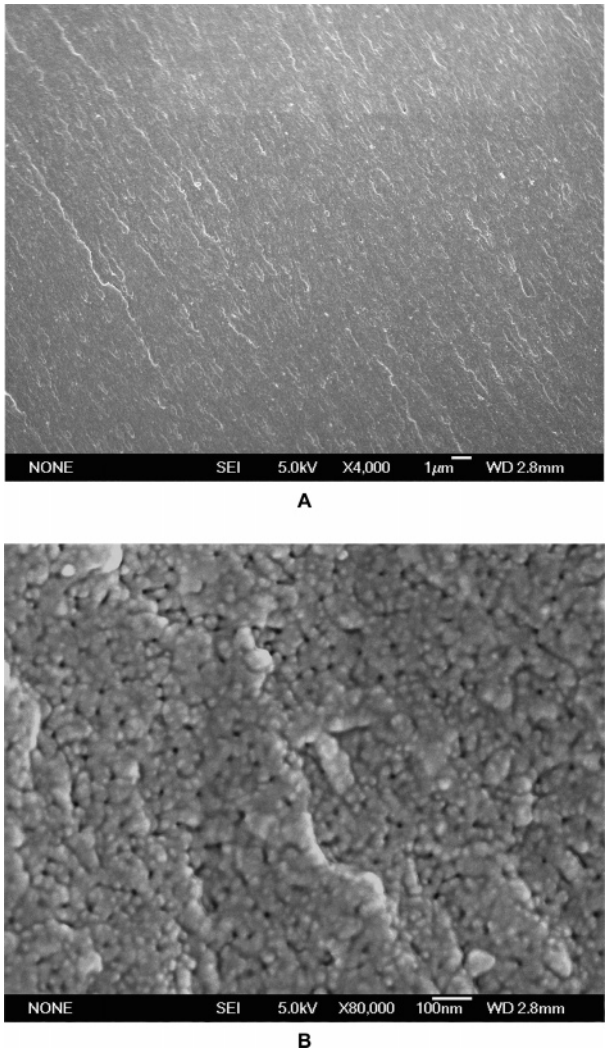

Figure 3. Micrographs of field emission scanning electron microscopy (FESEM) for the thermosets containing 10 wt % of PCL-*b*-PBA: (A) at the magnification of 4000×; (B) part A at the magnification of 80 000×.

The SAXS profiles of the thermosets containing 10, 20, 30, and 40 wt % of PCL-*b*-PBA diblock copolymer are shown in Figure 6. It is seen that the well-defined scattering peaks were observed in all the cases, indicating that the thermosets containing PCL-*b*-PBA are microphase-separated. In addition, it is noted that all the SAXS profiles possess the multiple scattering maxima as denoted with the arrows, indicating that the thermosets could possess long-range ordered microstructures. The positions of the scattering maxima remain essentially constant, apart from slight shifts to the higher q values with increasing the content of PCL-*b*-PBA. According to the position of the primary scattering peaks, the principal domain spacing d_m can be obtained to be 39.7, 36.9, 32.4, and 31.7 nm for the thermosets containing 10, 20, 30, and 40 wt % PCL-*b*-PBA

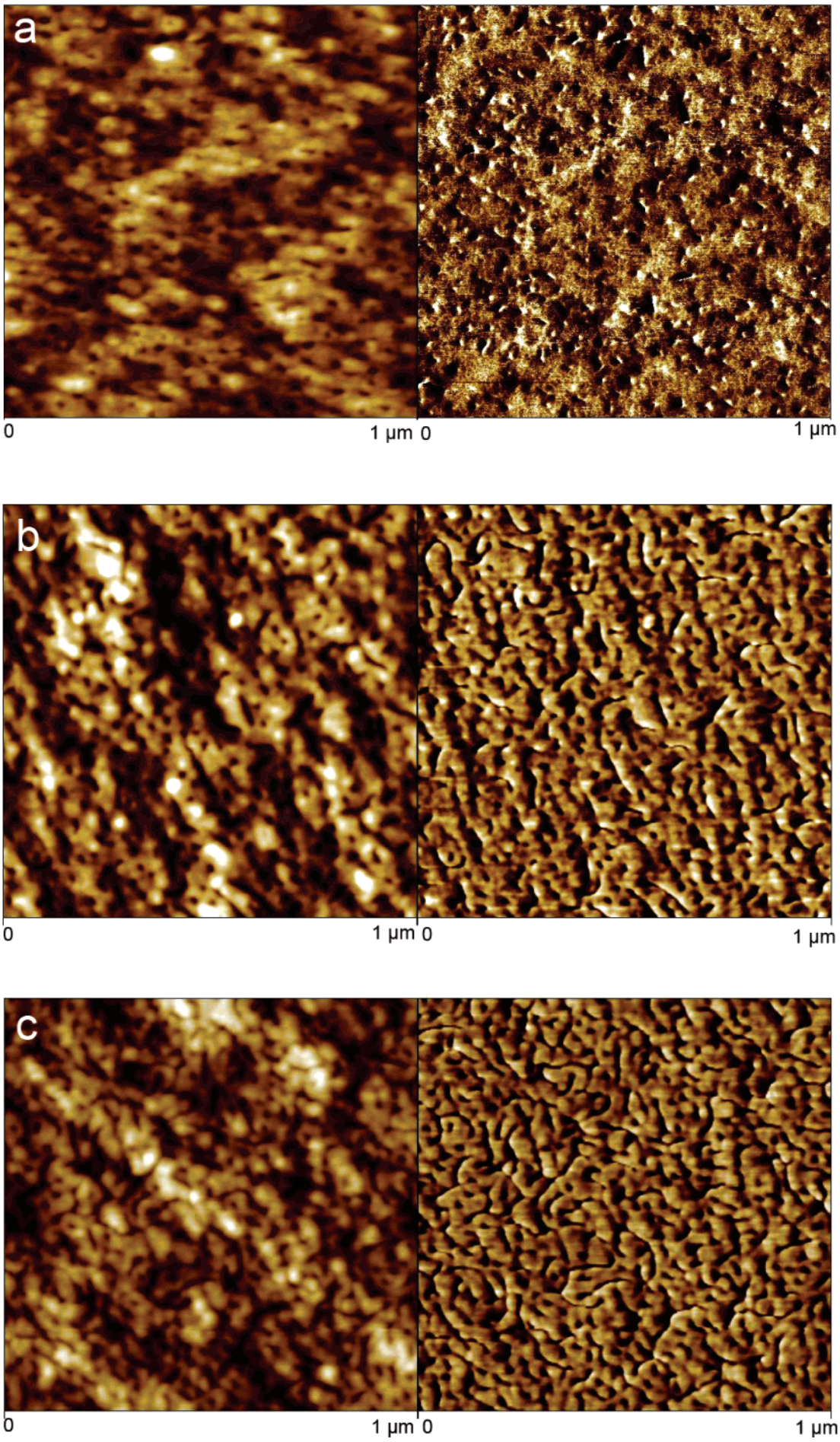
a
0
1 μm
0
1 μm
b
0
1 μm
0
1 μm
c
0
1 μm
0
1 μm

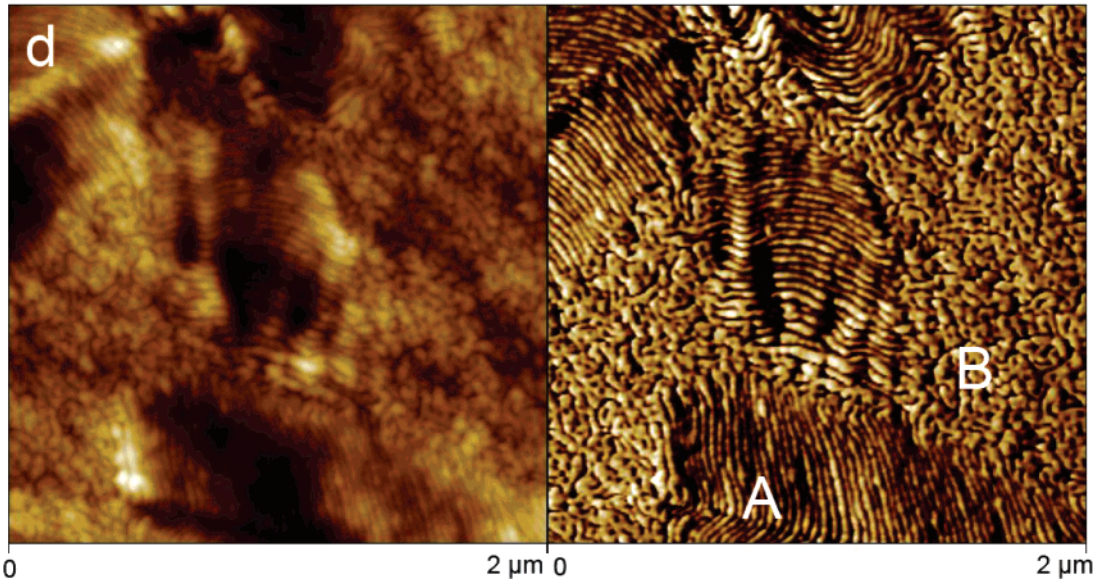

Figure 4. AFM images of the thermosets containing (a) 10, (b) 20, (c) 30, and (d) 40 wt % of PCL-*b*-PBA diblock copolymer. Left: topography; right: phase contrast images.

diblock copolymer, respectively. This result is in a good agreement with those obtained by means of FESEM and AFM. It is noted that the average distance between neighboring domains decreased with increasing the content of the diblock copolymer. The slight shifts of the scattering maxima could be associated with local rearrangement leading to an enhancement of the long-range order. The scattering peaks of the thermosets situated at q values of 1, $3^{0.5}$, and $9^{0.5}$ relative to the first-order scattering peak positions (q_m) are discernible. It is plausible to propose that these are the lattice scattering peaks of spherical (or cylindrical) nanophases arranged in cubic lattices such as body-centered cubic (bcc), face-centered cubic (fcc), or simple cubic symmetries. In addition, hexagonally packed cylinder morphology is also possible. It should be pointed out that it is not easy unambiguously to judge the types of packing lattices only in terms of SAXS profiles for the thermosetting blends containing 10, 20, and 30 wt % PCL-*b*-PBA since the scattering peaks are quite broad; i.e., the ordering is apparently not good enough. In fact, the thermosetting blend containing 40 wt % PCL-*b*-PBA displayed the combined lattices of lamellar and cubic symmetries as shown in the AFM micrograph.

Shown in Figure 7 are the DSC curves of the control epoxy, nanostructured epoxy thermosets, and PBA-*b*-PCL diblock copolymer. The glass transition temperature (T_g) of the control epoxy is about 153 °C. The curve of PCL-*b*-PBA diblock copolymer displays a sharp transition at ca. 56 °C, assignable to melting transition of PCL block. It is noted that all the thermosets investigated did not exhibit the melting transition of PCL blocks, suggesting that the PCL blocks were trapped in the thermosets; i.e., the PCL subchains are miscible with the epoxy networks.[10] The behavior of miscibility was further confirmed by the depression in glass transition temperatures (T_g's) for the epoxy-rich phases, as shown in Figure 7. In addition, it is worth noticing that the width of the glass transition region for the nanostructured thermosets is significantly broader than that of control epoxy. The broadening of the glass transition range could be attributed to the enrichment of soft PCL chains around the PBA microdomains; i.e., only the cross-linked epoxy matrices near the front of PBA domains were efficiently plasticized by PCL chains and exhibited the lower glass transition temperatures (T_g's) than the epoxy matrices that were not interpenetrated by PCL blocks. The miscibility is ascribed to the formation of the intermolecular hydrogen bonding interaction between the aromatic amine-cross-linked epoxy and PCL, which is readily evidenced by Fourier transform infrared spectroscopy (FTIR).

In Figure 8, the FTIR spectra of PCL-*b*-PBA and the nanostructured epoxy thermosets were presented in the range of 1680−1800 cm^{-1}. The absorption bands centered at 1735 cm^{-1} are ascribed to the stretching vibration of carbonyl groups (⟩C═O) in PCL and/or PBA blocks. In the spectra of the nanostructured thermosets, there appeared new shoulders at the lower frequency of 1706 cm^{-1}. The shoulder bands could be ascribed to the stretching vibration of the hydrogen-bonded carbonyls. The FTIR results indicate that the intermolecular hydrogen bonding interactions between the carbonyls of PCL (and/or PBA) and the hydroxyl groups of cross-linked epoxy networks were formed in the nanostructured thermosets. It should be pointed out that although both subchains (i.e., PCL and PBA) of the diblock copolymer possess carbonyl groups potential to form the intermolecular hydrogen bonding interactions with the hydroxyl groups of cross-linked epoxy networks, the degree of association of the two types of carbonyl groups with the hydroxyl groups of the epoxy matrix could be quite different. To investigate the difference in the intermolecular hydrogen bonding interactions, we prepared the binary thermosetting blends of epoxy with PCL and/or PBA. In these blends, both PCL and PBA possess the molecular weights identical with the subchain lengths of PCL and PBA in the diblock copolymer. Shown in Figure 9 are the FTIR spectra of the binary thermosetting blends containing 10 wt % PCL and/or PBA in the range of 1660−1800 cm^{-1}. It is of interest to note that the band of stretching vibration for PBA carbonyl groups at 1735 cm^{-1} are quite symmetrical, and no shoulder band at the lower frequencies is discernible. In contrast, the stretching vibration band of PCL in the binary blends of epoxy with PCL exhibited a pronounced shoulder component at 1706 cm^{-1}, suggesting that there are the intermolecular hydrogen bonding interactions between PCL and the cross-linked epoxy matrix. Therefore, it is plausible to propose that the shoulder bands at 1706 cm^{-1} for the nanostructured epoxy thermosets (Figure 8) result from the intermolecular hydrogen bonding interactions between the PCL subchains and the cross-linked epoxy matrix other than those between the PBA subchains and

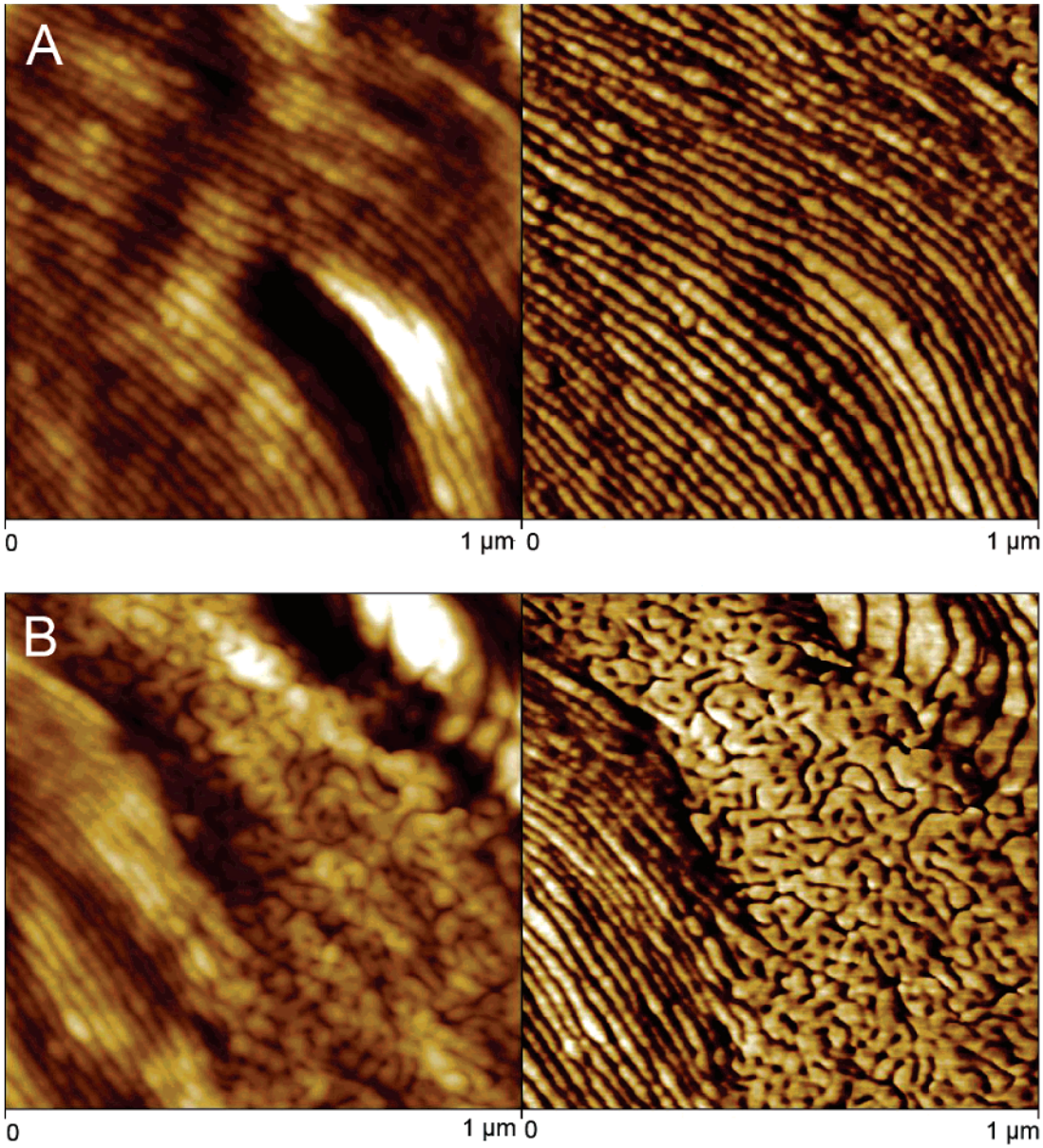

Figure 5. AFM images of the thermosets containing 40 wt % of PCL-*b*-PBA diblock copolymer. Left: topography; right: phase contrast images.

the cross-linked epoxy resin. In other words, the PBA could be microphase-separated out in the nanostructured epoxy thermosets while the PCL blocks are miscible with the epoxy matrices.

The nanostructured thermosets containing PCL-*b*-PBA were subjected to dynamic mechanical thermal analysis (DMTA). Shown in Figure 10 are the dynamic mechanical spectra of the nanocomposites. The MOCA-cured epoxy exhibited a well-defined relaxation peak (i.e., α transition) centered at ca. 160 °C, which is responsible for the glass−rubber transition of the cross-linked polymer. Apart from the α transition, the MOCA-cured epoxy exhibited a secondary transition (viz. β-relaxation) at the lower temperature (∼−60 °C). This transition is attributed predominantly to the motion of hydroxyl ether structural units [$-CH_2-CH(OH)-CH_2-O-$] and diphenyl groups in amine-cross-linked epoxy.[9] It is seen that upon adding PCL-*b*-PBA into the thermosets the α transition shifted to the lower temperatures. The T_g's of the epoxy matrix decreased with increasing the content of PCL-*b*-PBA diblock copolymer. The decreased T_g's are ascribed to the plasticization of PCL subchains of the block copolymer on the epoxy matrix. In addition, there appeared new transitions at −34 °C besides the α- and β-relaxations assignable to epoxy matrix; the intensity of the peaks increased with increasing the concentration of PCL-*b*-PBA. The new peaks are assignable to the glass transition of the PBA domains in the nanostructured thermosets. It should be pointed out that the transition at −34 °C is only assigned to PBA microdomains other than to the PCL blocks of the copolymer in the thermosets since PCL blocks are miscible with the MOCA-cross-linked epoxy. It has been judged that there are the intermolecular hydrogen bonding interactions between the PCL block and epoxy matrix in terms of Fourier transform infrared spectroscopy (FTIR).

Discussion

It is recognized that the formation of nanostructures can be carried out via self-assembly[3,5] or reaction-induced microphase separation mechanisms[4] of amphiphilic block copolymers in thermosets. In the protocol of self-assembly, the precursors of thermosets act as selective solvents of block copolymers and self-organized nanostructures (i.e., micelle) are formed prior to curing, and these disordered and/or ordered nanostructures are further locked in with the subsequent curing reaction. For the

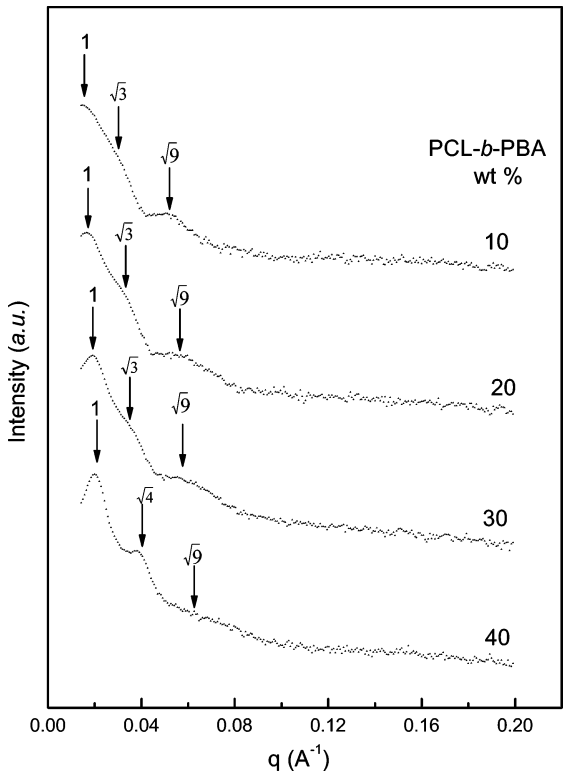

Figure 6. SAXS profiles of the thermosets containing PCL-*b*-PBA diblock copolymer. Each profile has been shifted vertically for clarity.

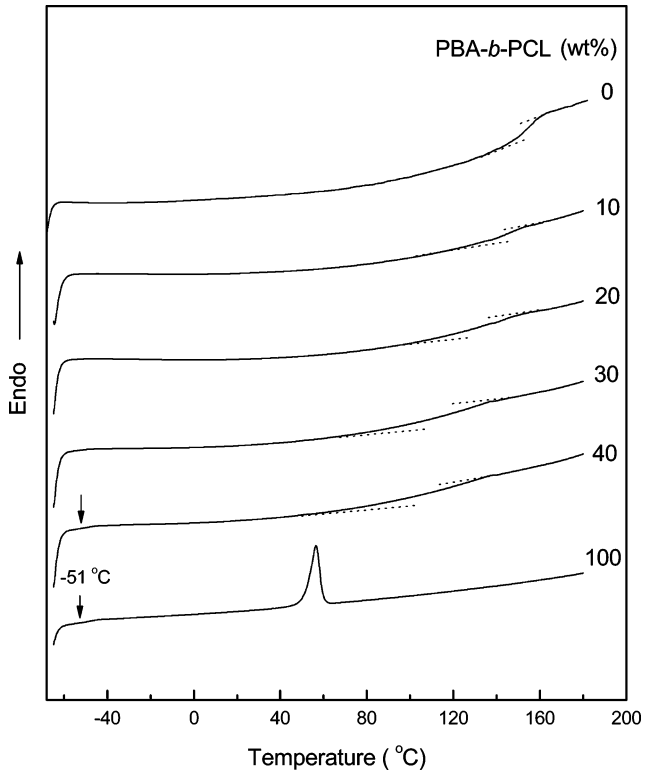

Figure 7. DSC curves of the control epoxy, PCL-*b*-PBA, and their nanostructured blends.

formation of nanostructures via reaction-induced microphase separation mechanism, it is required that all the subchains of the block copolymer are miscible with precursors of thermosets before curing whereas only a part of subchains were phase-separated from the matrix of thermosets after curing. In the present work, we designed and synthesized the PCL-*b*-PBA

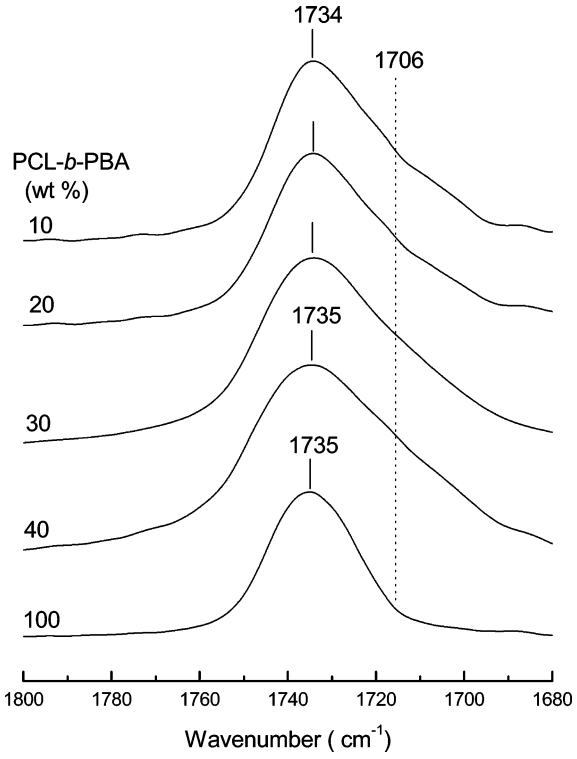

Figure 8. FTIR spectra of PCL-*b*-PBA diblock copolymer and the nanostructured thermosets. The spectrum of PCL-*b*-PBA diblock copolymer was obtained at 80 °C to melt the crystals of PCL subchain.

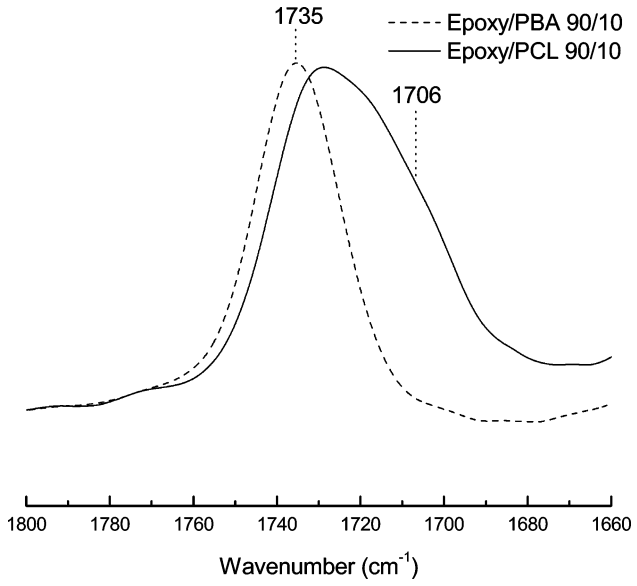

Figure 9. FTIR spectra of the binary epoxy and PCL (and/or PBA) blends in the range of 1660−1800 cm^{-1}.

diblock copolymer by knowing that (i) PCL is miscible with epoxy monomers before curing and also miscible with 4,4′-methylenebis(2-chloroaniline) (MOCA)-cured epoxy thermosets[2a,b,f−j,10] and (ii) the blend system composed of the low-molecular-weight PBA and epoxy precursors displayed an upper critical solution temperature (UCST) behavior and reaction-induced phase separation occurs when the blends are cured at elevated temperatures.

Before curing reaction, the miscibility (or solubility) of PCL and PBA with the precursors of epoxy resin (i.e., DGEBA and MOCA) was mainly ascribed to the nonnegligible entropic contribution of mixing (ΔS_m) to free energy of mixing (ΔG_m) since the epoxy precursor are low-molecular-weight compounds.

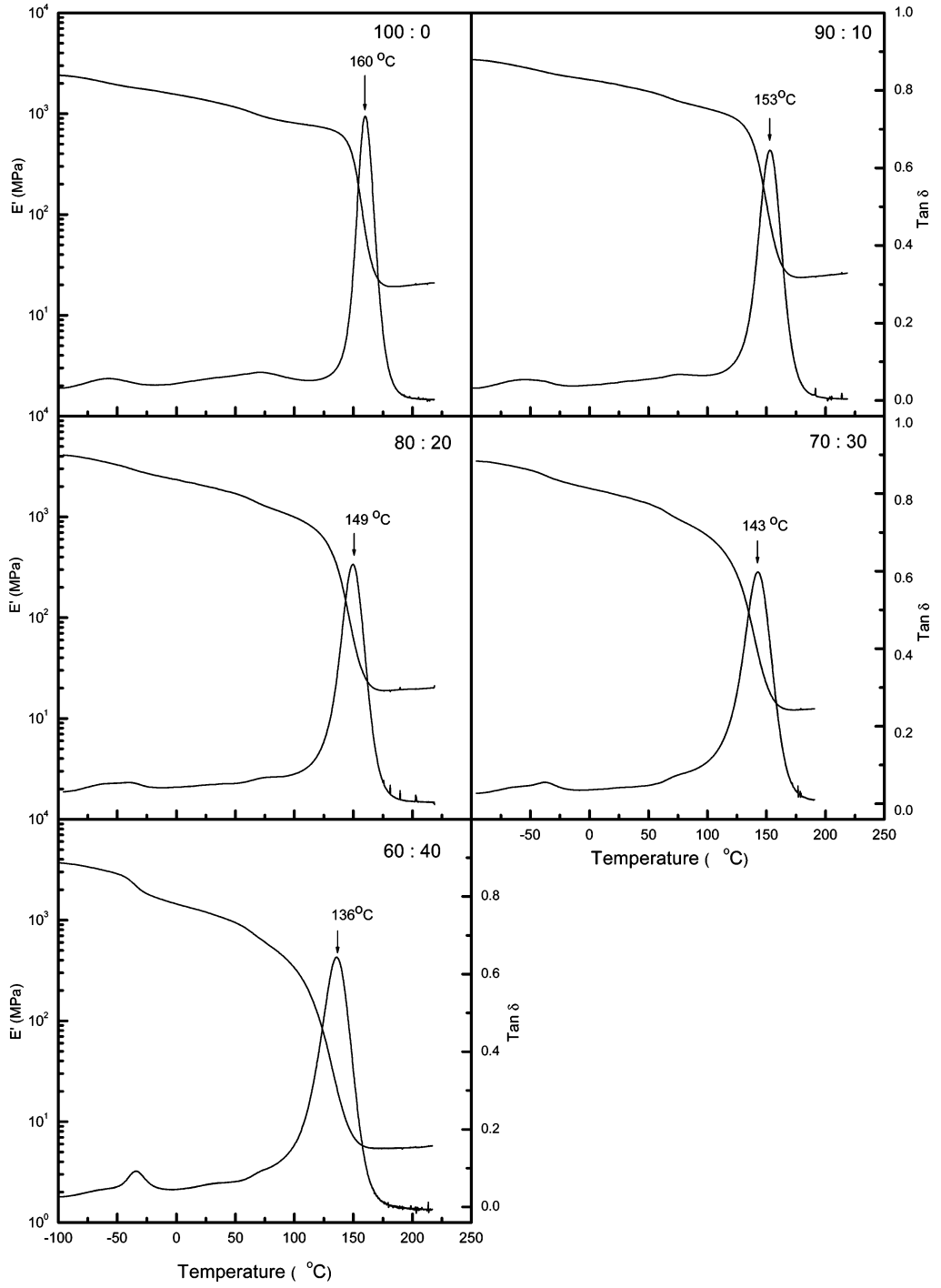

Figure 10. Dynamic mechanical spectra of the nanostructured epoxy thermosets.

After curing, the blends of epoxy resin with PCL displayed single, composition-dependent glass transition temperatures (T_g) in the entire composition as revealed by differential scanning calorimetry (DSC),[10] indicating that the cured blends are also miscible. The driving force for the miscibility of the thermosetting blends is ascribed to the formation of the intermolecular hydrogen bonding interactions between the aromatic amine-cross-linked epoxy and PCL. To know the miscibility of epoxy resin with the PBA block of PCL-*b*-PBA after and before curing reaction, we synthesized the PBA homopolymer with the degree of polymerization (M_n = 9900) comparable to the PBA subchain length in PCL-*b*-PBA. Before curing, the mixtures of the epoxy DGEBA and PBA were cloudy at room temperature. Upon heating the mixtures the system became transparent. This observation implies that the system displays the upper critical solution temperature (UCST) behavior. By means of phase contrast microscopy (PCM), the cloud point curve of the system was determined as shown in Figure 11. It is seen that the mixtures displayed an asymmetric phase diagram with the maximum critical solution temperature at ca. 78 °C when the content of PBA is about 30 wt %. It is worth noticing that the UCST is quite lower than 150 °C (i.e., the curing temperature), suggesting that when the mixtures are heated up to the curing temperature, the PBA will become miscible with DGEBA. In addition, it is observed that, with MOCA (the curing agent) being adding to the system, the homogeneity and transparency of system remained. The blends were cured at 150 °C for 2 h plus 180 °C for 2 h to access a complete curing reaction. It

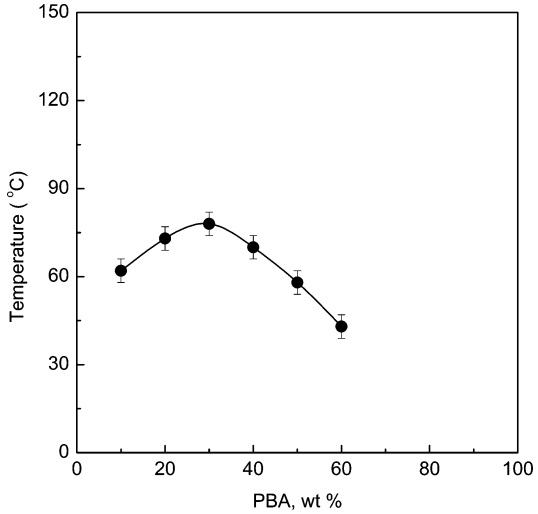

Figure 11. Cloud point curve of DGEBA/PBA blends.

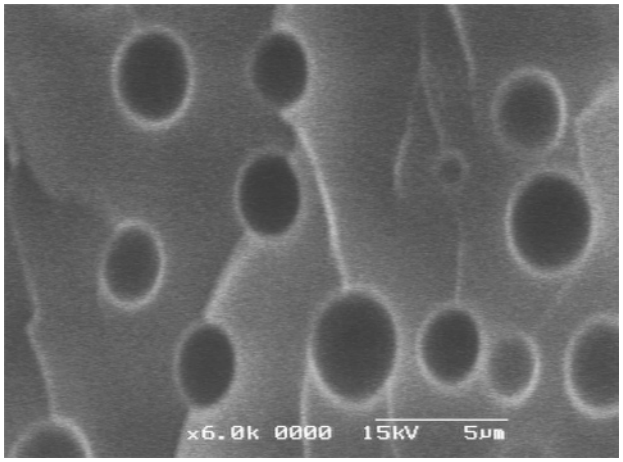

Figure 12. SEM micrograph of epoxy/PBA = 90/10 blends cured with MOCA. The fracture end of the blend has been etched with THF for 30 min.

was observed that with the curing reaction proceeding the system gradually became cloudy, implying the occurrence of the macroscopic reaction-induced phase separation. In order to investigate the morphology of the cured blends, the samples were fractured under cryogenic conditions using liquid nitrogen, the fractured ends were etched with the solvent THF, and the etched ends were subjected to the morphological observation using scanning electronic microscopy (SEM). Figure 12 representatively shows the SEM micrograph of the cured blends containing 10 wt % of PBA. It can be seen that the spherical holes with the size of 2−4 μm in diameter were uniformly dispersed in the continuous epoxy matrix after the PBA phase was rinsed by THF. This observation indicates that the PBA became immiscible with the MOCA-cross-linked epoxy resin after curing reaction. The driving force for the reaction-induced phase separation has been ascribed to the decrease of entropy of mixing resulting from polymerization.[1]

The knowledge of the miscibility and phase behavior of these binary systems after and before curing reaction is helpful for ones to understand the formation mechanism of the nanostructures in the thermosetting blends of epoxy resin with PCL-*b*-PBA diblock copolymer. It is plausible to propose that before curing reaction the self-organized nanostructures could be present at room temperature since the epoxy precursors are immiscible with the PBA blocks but miscible with the PCL blocks of the diblock copolymer at room temperature. Upon heating the system up to 150 °C, the self-reorganized structures were destroyed since the temperature exceeded the UCST of the mixtures of PBA with DGEBA. However, with the curing reaction proceeding, the PBA blocks were gradually microphase-separated out while the PCL blocks remained miscible with the epoxy matrix, and this process can be depicted in Scheme 2. It should be pointed out that the reaction-induced microphase separation of PBA blocks in the blends is quite different from the case of the PBA homopolymer with the comparable molecular weight in epoxy resin. The reaction-induced phase separation of homopolymer generally occurred at micrometer scale via spinodal decomposition (SD) (and/or nucleation and growth, NG) mechanism.[1] Nonetheless, when the PBA was covalently connected with a miscible block (i.e., an amphiphilic diblock copolymer is formed), phase separation would be carried out in a confined manner. In the present case, the PCL subchains of the diblock copolymer are miscible with the epoxy matrix; thus, the growth of PBA domains will be confined to the nanometer scale, and the macroscopic phase separation of PBA is thus suppressed by the presence of the PCL subchains. It is worth noticing that the size distribution of the PBA microdomains obtained is quite uniform. It is plausible to propose that the ordered nanostructures can be formed if the uniformly distributed PBA microdomains were densely packed. In the present case, the PBA microdomains were found to pack into a long-rang ordered nanostructures. The formation mechanism of the ordered nanostructure is in marked contrast to the mechanism of self-assembly of block copolymer in precursors of thermosets together with subsequent fixation of the self-organized structures.

Scheme 2. Formation of Lamellar Nanostructures in Epoxy Thermosets Containing PCL-*b*-PBA Diblock Copolymer

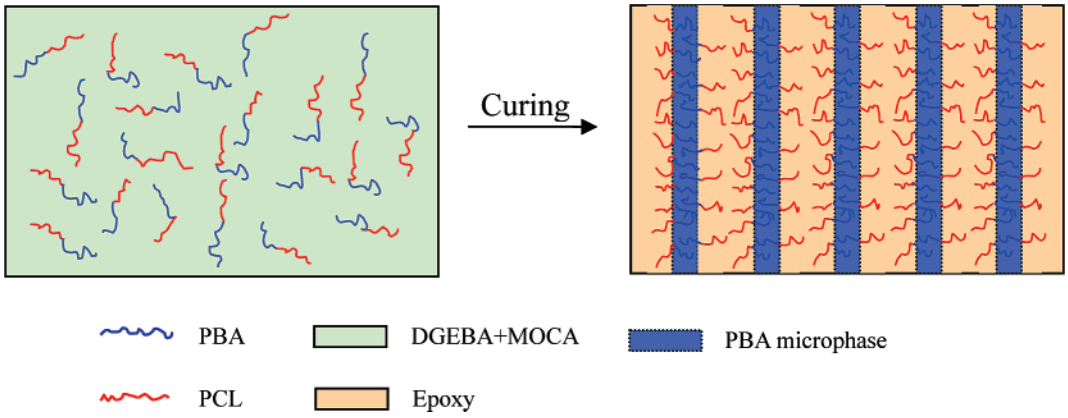

Conclusions

The diblock copolymer PCL-*b*-PBA was synthesized via the ring-opening polymerization (ROP) and atom transfer radical polymerization (ATRP). The PCL-*b*-PBA diblock copolymer was characterized by means of ^{1}H nuclear magnetic resonance spectroscopy (NMR) and gel permeation chromatography (GPC). The diblock copolymer was incorporated into epoxy thermosets to access the nanostructures in the thermosets. In terms of the miscibility of the subchains of the block copolymer with epoxy resin after and before curing reaction, it is judged that the nanostructures were formed via the mechanism of reaction-induced phase separation. The nanostructures were investigated by means of field emission scanning electron microscopy (FESEM), atomic force microscopy (AFM), small-angle X-ray scattering (SAXS), and dynamic mechanical analysis (DMA). It is found that, depending on the concentration of the diblock copolymer in the thermosets, the nanostructures from spherical particles to lamellar objects of PBA nanophases were obtained. The formation mechanism of the nanostructures is in marked contrast to the mechanism of self-organization of block copolymers and fixation of the self-organized structures in thermosets.

Acknowledgment. The financial support from the Natural Science foundation of China (Project No. 20474038 and 50390090) is acknowledged. S.Z. thanks the Shanghai Educational Development Foundation, China, under an award (2004-SG-18) to the "Shuguang Scholar".

References and Notes

(1) (a) Pascault, J. P.; Williams, R. J. J. In *Polymer Blends*; Paul, D. R., Bucknall, C. B., Eds.; Wiley: New York, 2000; Vol. 1, pp 379−415. (b) Guo, Q. In *Polymer Blends and Alloy*; Shonaik, G. O., Simon, G., Eds.; Marcel Dekker: New York, 1999; Chapter 6, pp 155−187.

(2) (a) Noshay, A.; Robeson, L. M. *J. Polym. Sci., Part A: Polym. Chem.* **1974**, *12*, 689. (b) Clark, J. N.; Daly, J. H.; Garton, A. *J. Appl. Polym. Sci.* **1984**, *29*, 3381. (c) Luo, X.; Zheng, S.; Zhang, N.; Ma, D. *Polymer* **1994**, *35*, 2619. (d) Zheng, S.; Zhang, N.; Luo, X.; Ma D. *Polymer* **1995**, *36*, 3609. (e) Zheng, H.; Zheng, S.; Guo, Q. *J. Polym. Sci., Part A: Polym. Chem.* **1998**, *35*, 3161. (f) Guo Q.; Harrats, C.; Groeninckx, G.; Koch, M. H. J. *Polymer* **2001**, *42*, 4127. (g) Guo, Q.; Harrats, C.; Groeninckx, G.; Reynaers, H.; Koch, M. H. J. *Polymer* **2001**, *42*, 6031. (h) Guo, Q.; Groeninckx, G. *Polymer* **2001**, *42*, 8647. (i) Zheng, S.; Lu, H.; Chen, C.; Nie, K.; Guo, Q. *Colloid Polym. Sci.* **2003**, *281*, 1015. (j) Zheng, S.; Zheng, H.; Guo, Q. *J. Polym. Sci., Part B: Polym. Phys.* **2003**, *41*, 1085.

(3) (a) Larrañaga, M.; Gabilondo, N.; Kortaberria, G.; Serrano, E.; Remiro, P.; Riccardi, C. C.; Mondragon, I. *Polymer* **2005**, *46*, 7082. (b) Meng, F.; Zheng, S.; Zhang, W.; Li, H.; Liang, Q. *Macromolecules* **2006**, *39*, 711. (c) Meng, F.; Zheng, S.; Li, H.; Liang, Q.; Liu, T. *Macromolecules* **2006**, *39*, 5072. (d) Meng, F.; Zheng, S.; Liu, T. *Polymer* **2006**, *47*, 7590. (e) Serrano, E.; Tercjak, A.; Kortaberria, G.; Pomposo, J. A.; Mecerreyes, D.; Zafeiropoulos, N. E.; Stamm, M.; Mondragon, I. *Macromolecules* **2006**, *39*, 2254.

(4) (a) Hillmyer, M. A.; Lipic, P. M.; Hajduk, D. A.; Almdal, K.; Bates, F. S. *J. Am. Chem. Soc.* **1997**, *119*, 2749. (b) Lipic, P. M.; Bates, F. S.; Hillmyer, M. A. *J. Am. Chem. Soc.* **1998**, *120*, 8963.

(5) (a) Mijovic, J.; Shen, M.; Sy, J. W.; Mondragon, I. *Macromolecules* **2000**, *33*, 5235. (b) Guo, Q.; Thomann, R.; Gronski, W. *Macromolecules* **2002**, *35*, 3133. (c) Guo, Q.; Thomann, R.; Gronski, W. *Macromolecules* **2003**, *36*, 3635. (d) Ritzenthaler, S.; Court, F.; Girard-Reydet, E.; Leibler, L.; Pascault, J. P. *Macromolecules* **2002**, *35*, 6245. (e) Ritzenthaler, S.; Court, F.; Girard-Reydet, E.; Leibler, L.; Pascault, J. P. *Macromolecules* **2003**, *36*, 118. (f) Kosonen, H.; Ruokolainen, J.; Nyholm, P.; Ikkala, O. *Macromolecules* **2001**, *34*, 3046. (g) Kosonen, H.; Ruokolainen, J.; Nyholm, P.; Ikkala, O. *Polymer* **2001**, *42*, 9481. (h) Grubbs, R B.; Dean, J. M.; Broz, M. E.; Bates, F. S. *Macromolecules* **2000**, *33*, 9522. (i) Kosonen, H.; Ruokolainen, J.; Torkkeli, M.; Serimaa, R.; Nyholm, P.; Ikkala, O. *Macromol. Chem. Phys.* **2002**, *203*, 388. (j) Rebizant, V.; Abetz, V.; Tournihac, T.; Court, F.; Leibler, L. *Macromolecules* **2003**, *36*, 9889. (k) Dean, J. M.; Verghese, N. E.; Pham, H. Q.; Bates, F. S. *Macromolecules* **2003**, *36*, 9267. (l) Rebizant, V.; Venet, A. S.; Tournillhac, F.; Girard-Reydet, E.; Navarro, C.; Pascault, J. P.; Leibler, L. *Macromolecules* **2004**, *37*, 8017. (m) Dean, J. M.; Grubbs, R. B.; Saad, W.; Cook, R. F.; Bates, F. S. *J. Polym. Sci., Part B: Polym. Phys.* **2003**, *41*, 2444. (n) Wu, J.; Thio, Y. S.; Bates, F. S. *J. Polym. Sci., Part B: Polym. Phys.* **2005**, *43*, 1950. (o) Guo, Q.; Dean, J. M.; Grubbs, R. B.; Bates, F. S. *J. Polym. Sci., Part B: Polym. Phys.* **2003**, *41*, 1994. (p) Thio, Y. S.; Wu, J.; Bates, F. S. *Macromolecules* **2006**, *39*, 7187.

(6) Wang, J. S.; Matyjaszewski, K. *J. Am. Chem. Soc.* **1995**, *117*, 5614.

(7) (a) Moineau, G.; Minet, M.; Dubois, P.; Teyssie, P.; Senninger, T. *Macromolecules* **1999**, *32*, 27. (b) Jnkova, K.; Chen, X.; Kops, J.; Batsberg, W. *Macromolecules* **1998**, *31*, 538. (c) Zhang, Q.; Remsen, E. E.; Wooley, K. L. *J. Am. Chem. Soc.* **2000**, *122*, 3642.

(8) Tanaka, H.; Nishi, T. *Phys. Rev. A* **1989**, *39*, 783.

(9) (a) Sanja, Z. N.; Kupehela, L. *Polym. Eng. Sci.* **1976**, *28*, 1149. (b) Ochi, M.; Okasaki, M.; Shimbo, M. *J. Polym. Sci., Part B: Polym. Phys.* **1982**, *20*, 89. (c) Shibanov, Y. D.; Godovsky, Y. K. *Prog. Colloid Polym. Sci.* **1989**, *80*, 110.

(10) (a) Yin, M.; Zheng, S. *Macromol. Chem. Phys.* **2005**, *206*, 929. (b) Ni, Y.; Zheng, S. *Polymer* **2005**, *46*, 5828.

MA062486V